

Mechanical Modeling and Analysis Based on Fine Drill



Kuikui Feng, Haodong Zhang, Qian Cheng, and Wuhong Wang

Abstract The main purpose of this paper is to study the change law of the contact condition between the fine drilling tool and the workpiece surface during cutting. Firstly, the structure of the drill tip of the fine drilling tool is analyzed, and the contact force of the drill tip is effectively decomposed. Then, on the basis of considering the cutting edge radius, the cutting mechanics model of each part of the drill tip was established according to the theory of slip line field. Finally, drilling experiments under different cutting conditions were carried out to solve the contact coefficient between the tool and the workpiece surface. The research shows that the high feed leads to greater ploughing effect in cutting, resulting in sharp change of contact force, which provides a research direction for tool tip design.

Keywords Fine drill · Main cutting edge · Chisel edge · Slip line field · Ploughing

1 Introduction

As an important part of aerospace engine, the injection plate is distributed with thousands of small holes. The size range of these holes belongs to the mesoscopic scale [1], and their geometric parameters play an important role in propellant injection performance and combustion stability in rocket engines. Therefore, it is of great

K. Feng · H. Zhang · Q. Cheng · W. Wang (✉)

Department of Industrial Engineering, Beijing Institute of Technology, Beijing 100081, PR China

e-mail: wangwh@bit.edu.cn

K. Feng

e-mail: fengkk1014@163.com

H. Zhang

e-mail: ZHDZYW@163.com

Q. Cheng

e-mail: billqiancheng@163.com

© The Author(s), under exclusive license to Springer Nature Singapore Pte Ltd. 2022

W. Wang et al. (eds.), *Green Connected Automated Transportation and Safety*,

Lecture Notes in Electrical Engineering 775,

https://doi.org/10.1007/978-981-16-5429-9_63

significance to establish the mechanical model and analyze its mechanical characteristics in the process of fine-hole cutting to improve the machining quality of injection plate and reduce the engine failure.

Fine drilling is essentially similar to conventional drilling and has many similarities in mechanical properties of cutting. However, the natural difference in the size magnitude also causes the mechanical properties to be different, which will be affected by the size effect [2], cutting edge radius [3], minimum cutting thickness [4] and other factors.

Abouridouane et al. [5] analyzed the scale effect in the cutting process of twist drill and established a three-dimensional FEM of ferrite-pearlite based C45 steel to study the influence law of cutting edge radius on chip shape. Lucca et al. [6] studied the relationship between plastic deformed layer, cutting edge radius and minimum cutting thickness in micro cutting, and found that the surface morphology of plastic deformed layer was independent of the minimum cutting thickness and only affected by the cutting edge radius. Malekian et al. [7] established the minimum chip thickness model based on the principle of minimum energy consumption and the infinite shear strain method, and then concluded that the cutting radius of the tool was positively correlated with the minimum chip thickness. Son et al. [8] established an ultra-precision cutting model and believed that the cutting edge radius and the friction coefficient should be considered to control the minimum chip thickness. Based on FEM, Vogler et al. [9] predicted that the minimum cutting thickness of pearlite and ferrite materials was 0.2 and 0.3 times of the radius of the blunt circle of the cutting edge, respectively. It can be seen that the cutting edge radius and the minimum cutting thickness are the important factors to determine the cutting quality of fine drill, and there is a close relationship between them. However, the cutting edge radius is dynamically changed under the action of force at all times in the cutting process. We need to carry on the mechanical analysis to the whole process of fine drilling cutting, in order to effectively monitor the tool state and predict the problems that will arise in fine drilling.

This paper focuses on the interaction between drill tip and borehole surface and its effect on material properties. In this paper, a mechanical model of fine drill based on time is established to analyze the contact force of each part of the drill tip, especially the change of the drilling force at the cutting edge when the cutting tool is worn. Through the analysis of the experimental data, the contact coefficient of the cutting deformation zone was solved, and the relationship between the tool wear and the contact force was evaluated.

2 Experimental Setup

The cutting force of the tool in the drilling process was measured experimentally to verify the mechanical model of fine drilling in this study. Figure 1 show the schematic diagram of the experimental device. We Prepared a 1Cr18Ni9Ti stainless steel sample, the size is $\varnothing 100 \times 4$ mm, placed it in the table of the Kistler 9275

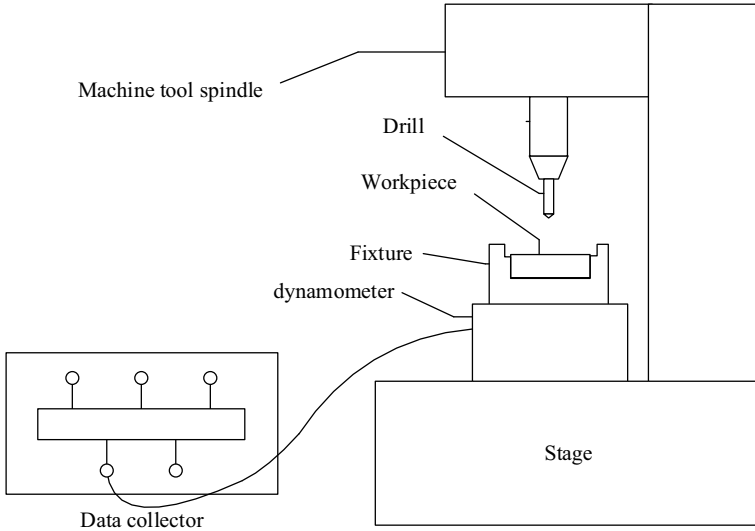


Fig. 1 Diagram of cutting experimental

Table 1 Parameters of tool

Cutting diameter	Chisel diameter	Blade angle
1 mm	0.3 mm	118°
Feed	Cutting speed	Rotate speed
5 $\mu\text{m}/\text{rev}$	18.8 m/min	6000 r/min

dynamometer in desktop on the dynamometer. The material of drill is carbide, its parameters are shown in Table 1.

3 Cutting Process Analysis

In the fine drilling process, the cutting part of the drill tip is composed of two parts, namely the main cutting edge and the chisel edge (Fig. 2). The main cutting edge is the intersecting line of the spiral groove and the flank, which is used for oblique cutting of the workpiece. The chisel edge is the intersection line between the rake face and the flank face, showing a slightly curved S-shape. Therefore, the cutting process of fine drilling is divided into five stages [10]. The 0– t_1 stage: The chisel cutting edge orthogonal cutting workpiece; The t_1 – t_2 stage: The main cutting edge oblique cutting material; The t_2 – t_3 stage: The drill tip is drilled into the workpiece completely, and the workpiece is acted on by two parts of cutting force. The t_3 – t_4 stage: Part of the chisel edge drill through the workpiece; The t_4 – t_5 stage: The chisel edge and part of the main cutting edge drill through the workpiece, and the workpiece

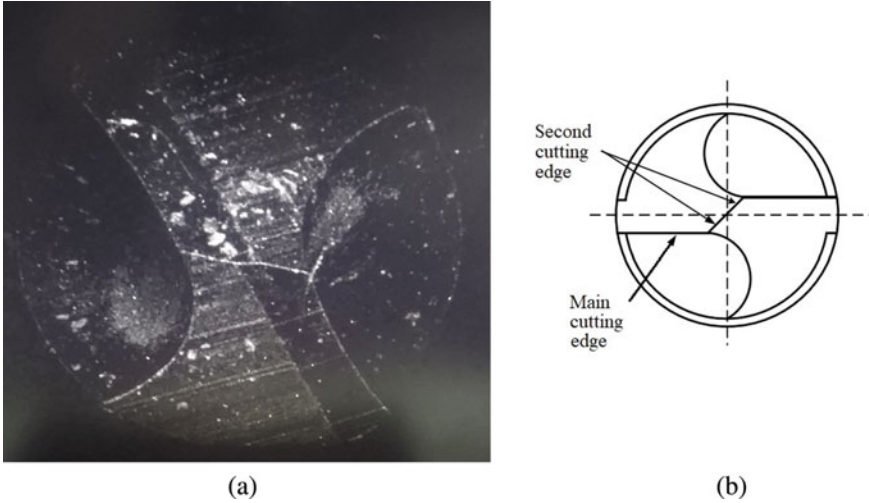


Fig. 2 Drill tip. a Entity, b structure

is only subjected to part of the cutting force of the main cutting edge until the cutting force is completely eliminated at the time of t_5 . So the cutting force model of five stages can be established, as follows in Eq. (1):

$$F_c(t) = \begin{cases} \frac{t}{t_1} F_s, & 0 < t < t_1 \\ F_s + \frac{t - t_1}{t_2 - t_1} F_m, & t_1 < t < t_2 \\ F_s + F_m, & t_2 < t < t_3 \\ \frac{t_4 - t}{t_4 - t_3} F_s + F_m, & t_3 < t < t_4 \\ F_s + \frac{t_5 - t}{t_5 - t_4} F_m, & t_4 < t < t_5 \end{cases} \quad (1)$$

where F_m and F_s are respectively the cutting forces of the main cutting edge and the chisel edge. Therefore, we can first establish the cutting force model of the two parts of the drill tip, and then solve the cutting force model based on time.

3.1 The Main Cutting Edge

The cutting process of the main cutting edge is oblique cutting (Fig. 3). The included Angle between the cutting direction and the chisel edge is the half peak angle φ , the thickness of the drilling core is r_w , and the distance between point a on the cutting

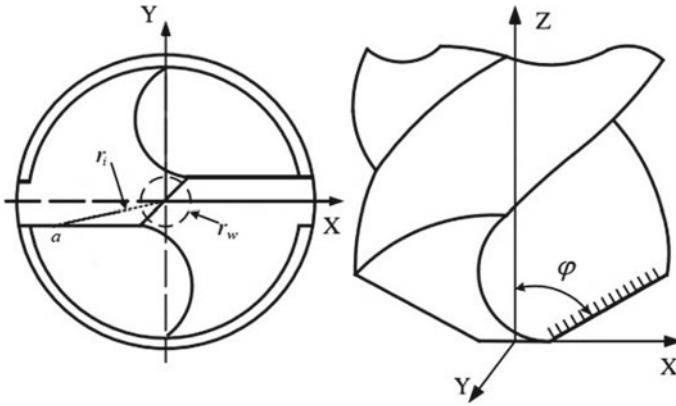


Fig. 3 The structure of main cutting edge

edge and the drilling shaft is r_i . The main cutting edge can be divided into several cutting units, and the cutting force of each cutting unit can be calculated according to the mechanical modeling method of Chandrasekharan et al. [11]. Then the cutting force acting on the workpiece is the superposition of the cutting force vectors of all the cutting units. Considering that the cutting thickness of fine drilling cutting is small, the cutting edge should be regarded as a circular arc. According to the slip line field theory, oblique cutting slip line field model [12] of the main cutting edge is established, as shown in Fig. 4.

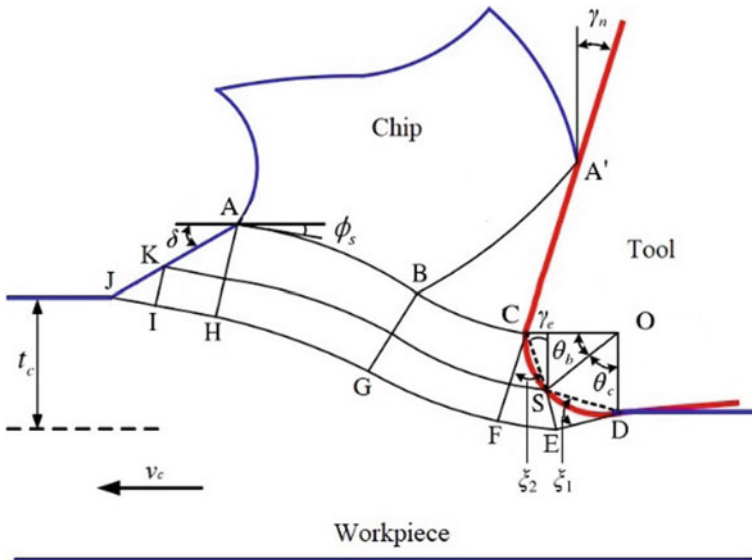


Fig. 4 Slip line field model of cutting element on main cutting edge

The model is divided into three plastic deformation zones [13]: the first shear plane region, ABCFGHIJK, the second deformation friction zone A'BC and the third deformation friction zone CSDEF. Surface CS and SD are edge contact surfaces, and their included angles with slip lines DE and CF are respectively ξ_1 and ξ_2 ; The central angles are respectively θ_b and θ_c ; The front Angle between AKJ and the horizontal plane is δ ; The shearing Angle between curve AB and the horizontal plane is ϕ_s ; The effective front Angle between CS and the vertical plane is γ_e ; The normal forward Angle between the rake face and the vertical plane is γ_n ; The radius of the drill tip is r_c .

The contact length between drill tip and workpiece are given as

$$\begin{cases} l_{CS} = 2r_c \sin\left(\frac{\pi}{4} + \frac{\gamma_n}{2} - \frac{\theta_c}{2}\right) \\ l_{SD} = 2r_c \sin \frac{\theta_c}{2} \end{cases} \quad (2)$$

The feed is f , so the thickness of the undeformed chip is given by

$$t_c = 0.5f \sqrt{\frac{r_i^2 - r_w^2}{r_i^2(1 + \cos^2 \varphi) - r_w^2}} \quad (3)$$

The contact length between the rake face and the chip:

$$l_{A'C} = \frac{t_c + \sqrt{2}(l_{CS} \cos \xi_2 + l_{SD} \sin \xi_1) \sin \delta - r_c(1 + \sin \gamma_e)}{\sin \phi_s} \quad (4)$$

The cutting force perpendicular to the cutting edge plane on the cutting element is

$$dF_m = k_s(k_{A'}l_{A'C} + k_C l_{CS} + k_S l_{SD}) \quad (5)$$

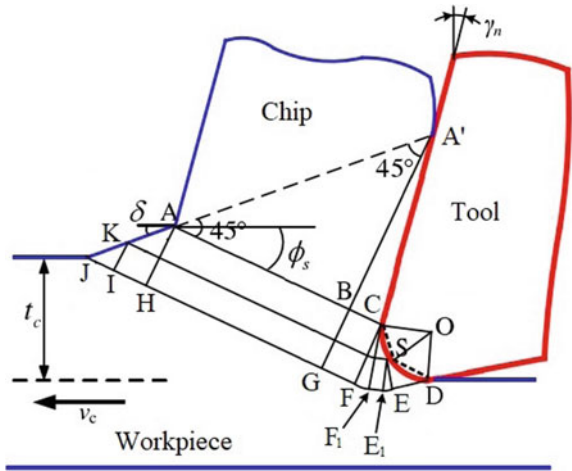
where k_s is the shear flow stress; $k_{A'}$, k_C and k_S are the contact coefficients between the tool and contact surface, respectively.

The axial cutting force F_m on the main cutting edge as follows:

$$F_m = (D - D_c)dF_m \cos \varphi \quad (6)$$

where D is the diameter of cutting tool; D_c is the diameter of chisel edge.

Fig. 5 Slip line field model of cutting element on second cutting edge



3.2 The Chisel Edge

Similarly, the chisel edge is equally divided into multiple cutting elements, and the cutting force acting on the workpiece is the superposition of the cutting force vectors of all the cutting elements. The orthogonal slip line field model of the chisel edge is shown in Fig. 5.

As in the model of the main cutting edge, the chisel edge is still divided into three plastic deformation zones. According to Eqs. (2)–(4), the contact length between the tool and the material is solved. Since the chisel edge is perpendicular to the cutting direction, the half peak Angle of the drill tip is $\varphi = 90^\circ$, and the thickness of unchipping t_c is $0.5f$. So $l_{A'C}$ is different. As the friction zone between the flank face and the workpiece have other zone-CFF1 and SEE1, ξ_1 and ξ_2 are reduced.

According to Eq. (5), We could calculate the cutting force of the cutting unit, then the axial cutting force on the chisel edge of the fine drill as follows:

$$F_s(t) = D_c d F_s \tag{7}$$

3.3 Cutting Force Experiment

The cutting heat generated by cutting will aggravate the tool wear and increase the radius of cutting edge, resulting in the undeformed chip thickness less than the minimum chip thickness and a large number of elastic deformation of the workpiece. The contact force is generated by ploughing and the tool contact coefficient will change at this time. Therefore, the cutting edge of the tool is actually dynamic, but in this example, it is assumed to be a constant value.

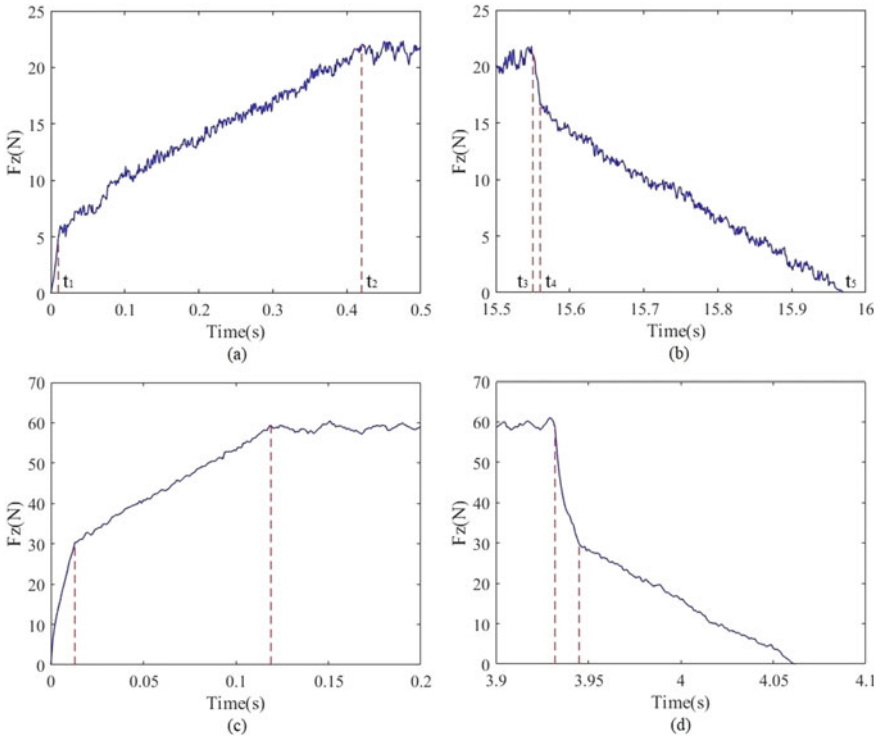


Fig. 6 The thrust value at low feed and high speed **a** $f = 5 \mu\text{m/rev}$ drilling in; **b** $f = 5 \mu\text{m/rev}$ drilling out; **c** $f = 20 \mu\text{m/rev}$ drilling in; **d** $f = 20 \mu\text{m/rev}$ drilling out

In order to calculate the cutting force of the tool in the cutting process, the unknown indentation half Angle and the contact coefficients need to be determined by micro-drilling experiments. We carried out cutting force experiments at constant rotational speed ($n = 6000 \text{ rpm}$) and different feed rates ($f = 5\text{--}20 \mu\text{m/rev}$). Figure 6 shows the thrust values for low and high feed cutting with an initial edge radius of $3 \mu\text{m}$. The chisel edge is drilled into the workpiece in a very short period of time, resulting in a very rapid increase in thrust, while the main cutting edge thrust increases slowly and remains stable after the bit is fully drilled. The thrust fluctuation value of the tool is large and the main cutting edge plays the leading role at low feed condition. It is related to the vibration in the cutting process. As the feed rate increases, the thrust value of the transverse cutting edge will become larger and larger, and even tends to exceed the main cutting edge, which is consistent with the description of Anish et al. [14]. It shows that with the increasing of tool temperature and wear, the contact conditions between the drill tip and the workpiece are changed, which affects the thrust measurement value.

Based on thrust measurements from fine drilling experiments under different conditions and the mechanical models of each area in Sect. 3, the contact coefficients

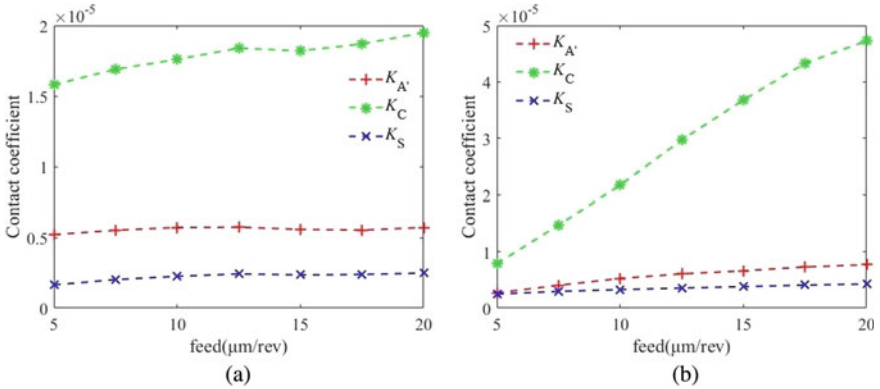


Fig. 7 Contact coefficient of tool-workpiece. **a** The main cutting edge, **b** the chisel edge

between the main cutting edge and the chisel edge of the drill tip and the contact surface can be determined by combining.

Figure 7 shows that no matter the main cutting edge or the chisel edge, the contact coefficient is much higher than the other two contact coefficients at different feed, which indicates that the resistance of the tool mainly concentrates on the intersection of the rake face and the flank face—the material shear area. With the increase of feed, the contact coefficients of main cutting edge and chisel edge trend. However, the thrust of chisel edge rise rapidly in a very short time, gathered in the energy. So the center part have serious ploughing phenomenon, which makes the chip more difficult to form. It is why the contact coefficient of chisel edge increases significantly faster. In this case, the tool wear is serious; the cutting edge radius r_c is increased; and the contact force is further improved. It also confirms the chisel edge thrust growth faster than the main cutting edge.

Therefore, when we design the structure of fine drill, we should appropriately reduce the diameter of the chisel edge to prevent chip accumulation on the basis of maintaining the tool stiffness.

4 Conclusions

- (1) Based on the consideration of the cutting edge radius, this paper analyzes the mechanical problem of the drill tip in the dry drilling process of stainless steel 1Cr18Ni9Ti sample, and puts forward an instantaneous mechanical model to predict the change law of the cutler-workpiece contact force and contact coefficient with the feed amount. The results show that the high feed increases the complexity of the contact conditions between the tool and the workpiece surface.

- (2) The contact coefficient at the intersection of the rake face and the flank face plays a leading role in the contact force of the whole tool. It is necessary to fully consider the local overheating caused by chip accumulation in the tool design, and reduce the width of chisel edge appropriately.

References

1. Zmijanovic V, Leger L, Depussay E, Sellam M, Chpoun A (2016) Experimental–numerical parametric investigation of a rocket nozzle secondary injection thrust vectoring. *J Propul Power* 32(1):196–213
2. Sabana A, Soumya G, Sankar MS, Rinku KM, Anandita S, Ramesh KS (2019) Study of cutting forces and surface integrity in micro drilling of a Ni-based super alloy. *J Manuf Process* 45:368–378
3. Abdellaoui L, Khelifi H, Sai WB, Hamdi H (2020) Tool nose radius effects in turning process. *Mach Sci Technol* 25(1):1–30
4. Aslantas K, Alatrushi LKH, Bedir F, Kaynak Y, Yilmaz N (2020) An experimental analysis of minimum chip thickness in micro-milling of two different titanium alloys. *Proc Inst Mech Eng Part B J Eng Manuf* 234(12):1486–1498
5. Abouridouane M, Klocke F, Lung D et al (2012) Size effects in micro drilling ferritic–pearlitic carbon steels. *Proc CIRP* 3:91–96
6. Lucca DA, Rhorer RL, Komanduri (1991) Energy dissipation in the ultra-precision machining of copper. *Annals CIRP* 40(1):69–72
7. Malekian M, Mostofa MG, Park SS et al (2011) Modeling of minimum uncut chip thickness in micro machining of aluminum. *J Mater Process Technol* 5:1–7
8. Son SM, Lim HS, Ahn JH (2005) Effects of the friction coefficient on the minimum cutting thickness in micro-cutting. *Int J Mach Tools Manuf* 45:529–535
9. Vogler MP, DeVor RE, Kapoor SG (2004) On the modeling and analysis of machining performance in micro-endmilling, part I: surface generation. *J Manuf Sci Eng* 126(4):685
10. Karpat Y, Karagüzel U, Bahtiyar O (2020) A thermo-mechanical model of drill margin-borehole surface interface contact conditions in dry drilling of thick CFRP laminates. *Int J Mach Tools Manuf* 154:103565
11. Chandrasekharan V, Kapoor SG, Devor RE (1995) A mechanistic model to predict the cutting forces in drilling: with application to fiber reinforced composite materials. *J Eng Ind* 117:559–570
12. Sambhav K, Tandon P, Kapoor SG, Dhande SG (2013) Mathematical modeling of cutting forces in microdrilling. *J Mech Sci Technol* 135(1):014501
13. Fang N (2003) Slip-line modeling of machining with a rounded-edge tool—Part I: new model and theory. *J Mech Phys Solids* 51(4):715–742
14. Paul A, Kapoor SG, DeVor RE (2005) A chisel edge model for arbitrary drill point geometry. *J Manuf Sci Eng* 127:23–32